

## Theory of Coulomb drag in graphene

Wang-Kong Tse,<sup>1</sup> Ben Yu-Kuang Hu,<sup>1,2</sup> and S. Das Sarma<sup>1</sup>

<sup>1</sup>Condensed Matter Theory Center, Department of Physics, University of Maryland, College Park, Maryland 20742, USA

<sup>2</sup>Department of Physics, University of Akron, Akron, Ohio 44325-4001, USA

(Received 26 April 2007; published 6 August 2007)

We study the Coulomb drag between two single graphene sheets in intrinsic and extrinsic graphene systems with no interlayer tunneling. The general expression for the nonlinear susceptibility appropriate for single-layer graphene systems is derived using the diagrammatic perturbation theory, and the corresponding exact zero-temperature expression is obtained analytically. We find that, despite the existence of a nonzero conductivity in an intrinsic graphene layer, the Coulomb drag between intrinsic graphene layers vanishes at all temperatures. In extrinsic systems, we obtain numerical results and an approximate analytical result for the drag resistivity  $\rho_D$ , and find that  $\rho_D$  goes as  $T^2$  at low temperature  $T$ , as  $1/d^4$  for large layer separation  $d$ , and  $1/n^3$  for high carrier density  $n$ . We also discuss qualitatively the effect of plasmon-induced enhancement on the Coulomb drag, which should occur at a temperature of the order of or higher than the Fermi temperature.

DOI: 10.1103/PhysRevB.76.081401

PACS number(s): 73.40.-c, 73.21.Ac, 73.63.Bd

**Introduction.** With the recent advent of the experimental fabrication of a single layer of graphene, the electronic and transport properties of this newly discovered material have been intensively studied both experimentally<sup>1,2</sup> and theoretically.<sup>2-4</sup> Whereas electronic structure experiments have revealed detailed subtle many-body effects on the graphene energy spectrum, transport experiments on graphene have also revealed some unusual features, most noticeably, the nonzero minimum conductivity around zero bias gate voltage.<sup>1</sup> Up to now, the transport experiments performed have been focused only on the longitudinal and Hall transport properties<sup>1,5</sup> (in both weak and strong magnetic fields, including the quantum Hall regime) and weak localization.<sup>6</sup> All these phenomena depend on the physics of scattering of individual single quasiparticle from impurities, with electron-electron many-body interaction effects playing a quantitatively minor role. In two-dimensional electron gas (2DEG) semiconductor double-layer structures (e.g., modulation-doped GaAs/Al<sub>x</sub>Ga<sub>1-x</sub>As double quantum wells), electron-electron scattering between the 2DEG layers gives rise to the Coulomb drag effect, where a “drag” current is induced purely from the momentum exchanges through interlayer electron-electron scattering events.<sup>7-9</sup> One measures the effect of Coulomb drag by the drag resistivity defined by  $\rho_D = E_{\text{pas}}/J_{\text{act}}$ , where  $E_{\text{pas}}$  is the drag electric field in the open-circuited passive layer and  $J_{\text{act}}$  is the current density in the active layer. In high-mobility samples where the disorder is weak,  $\rho_D$  goes as  $T^2$  at low temperatures  $T$ , and as  $d^{-4}$  for large double-layer separation  $d$  (see Refs. 7 and 10).

In this paper, we investigate the Coulomb drag in graphene double-layer systems, considering both the intrinsic [chemical potential  $\mu = \varepsilon_{\text{Dirac pt.}}$  (=0 in this paper)] and extrinsic ( $\mu \neq 0$ ) cases. So that there is no semantic confusion in what we mean by double-layer graphene, we emphasize that in our terminology “double-layer” means two *isolated* parallel two-dimensional (2D) monolayers separated by a distance  $d$ , with *no* interlayer tunneling. The electronic structure of each graphene monolayer is thus unaffected by the other, and each graphene layer is assumed to have its own variable carrier density in the extrinsic case. Our system is thus different from the ordinary “bilayer” graphene where  $d \sim 1-5$  Å with strong interlayer tunneling. Throughout this

paper, we shall also use the terms “undoped” and “doped” interchangeably with “intrinsic” and “extrinsic” respectively, keeping in mind that in experiments  $\mu$  can be changed by both chemical doping and gating with an applied voltage. The Coulomb drag in graphene is interesting not only because it is a novel material with a linear energy spectrum, but also because it only spans a thickness of a single carbon atom. Hence the electrons are much more confined along the perpendicular direction compared to a 2DEG in a quantum well, where the finite width thickness has to be taken into account in any quantitative comparison with experiments. Thus the Coulomb drag phenomenon in graphene is expected to be theoretically very well accounted for with two zero-thickness graphene sheets. In addition, tunneling is only appreciable when the the out-of-plane  $\pi$  orbitals from the two graphene sheets start to overlap with each other at an interlayer distance  $d$  of a few angstroms ( $d \approx 3.5$  Å in naturally occurring graphite), making it possible to study the effect of Coulomb drag for an interlayer separation  $d$  down to a few tens of angstroms, about an order of magnitude smaller than is possible in the usual double quantum well systems without appreciable tunneling.

**Theory.** Graphene has a real-space honeycomb lattice structure with two interpenetrating sublattices, giving a hexagonal Brillouin zone. At each of the corners of the Brillouin zone, denoted as  $K$  or  $K'$ , the energy dispersion is linear and the effective low-energy Hamiltonian in the vicinity of these points is given by  $H_0 = v \hat{\sigma} \cdot \mathbf{k}$ , where  $\hat{\sigma}$  are the Pauli spin matrices,  $\mathbf{k} = (k_x, k_y)$  is the wave vector relative to  $K$  or  $K'$ , and  $v \approx 10^6$  m/s. The eigenenergy is  $\epsilon_{k\lambda} = \lambda v |\mathbf{k}|$ , where the chirality label  $\lambda = \pm 1$  describes conduction band ( $\lambda = 1$ ) and valence band ( $\lambda = -1$ ) spectra. Throughout this paper we let  $\hbar = 1$  unless it is written out explicitly.

The drag conductivity, in the lowest leading order in the interlayer potential, is given by<sup>11-13</sup>

$$\sigma_D = \frac{1}{16\pi k_B T} \sum_q \int_0^\infty d\omega \frac{\Gamma_1(q, \omega) \Gamma_2(q, \omega) |U_{12}(q, \omega)|^2}{\sinh^2(\hbar\omega/2k_B T)}, \quad (1)$$

where subscripts “1” and “2” are the labels for the two single-layer graphene,  $\Gamma_i$  is the nonlinear susceptibility for

layer  $i$ , and  $U_{12}$  is the screened interlayer potential in the random phase approximation (RPA).<sup>11,12</sup> In experiments, one measures the drag resistivity, which is obtained from the drag conductivity as  $\rho_D = -\sigma_D / (\sigma_{L1}\sigma_{L2} - \sigma_D^2) \approx -\sigma_D / \sigma_{L1}\sigma_{L2}$ , where  $\sigma_{Li}$  is the longitudinal conductivity of the individual layer  $i$ .

In this paper, we restrict ourselves to the Boltzmann regime ( $\omega\tau \gg 1$  or  $ql \gg 1$ , where  $l = v\tau$  is the mean free path) corresponding to weak impurity scattering, which is relevant to actual experimental situations where high-mobility samples with dilute impurities are used. The longitudinal current for the graphene Hamiltonian is  $\mathbf{J} = e\partial H_0 / \partial \mathbf{k} = ev\hat{\sigma}$ . In the presence of impurities, vertex correction to the current is taken into account within the impurity ladder approximation, which gives the impurity-dressed current vertex as  $\mathbf{J} = (\tau_{tr}/\tau)ev\hat{\sigma}$ , where  $\tau_{tr}$  is the transport time for graphene.

The central quantity in the Coulomb drag problem is the nonlinear susceptibility,<sup>11-13</sup>  $\Gamma$ . Following Ref. 13, we express the nonlinear susceptibility as (we denote the  $x$  components of  $\Gamma$  and  $\mathbf{J}$  simply as  $\Gamma$  and  $J$ )

$$\Gamma(\mathbf{q}, \omega) = \tau \sum_{\lambda, \lambda' = \pm} \sum_{\mathbf{k}} [\tilde{J}_{\lambda\lambda}(\mathbf{k} + \mathbf{q}) - \tilde{J}_{\lambda'\lambda'}(\mathbf{k})] \times \text{Im} \left\{ (1 + \lambda\lambda' \cos \theta_+) \frac{n_F(\epsilon_{k\lambda'}) - n_F(\epsilon_{k+q\lambda})}{\omega + \epsilon_{k\lambda'} - \epsilon_{k+q\lambda} + i0^+} \right\}, \quad (2)$$

where  $\tilde{J}(\mathbf{k}) = U_k^\dagger J U_k$  is the impurity-dressed charge current vertex expressed in the chiral basis and  $\theta_+ = \phi_{\mathbf{k}+\mathbf{q}} - \phi_{\mathbf{k}}$  is the scattering angle from momentum  $\mathbf{k}$  to  $\mathbf{k} + \mathbf{q}$ . Equation (2) is different from the nonlinear susceptibility for a regular 2DEG with quadratic spectrum in two ways: (i) there are contributions to the electron-hole excitations coming from intraband transitions ( $\lambda = \lambda'$ ) and interband transitions ( $\lambda \neq \lambda'$ ); (ii) there is an additional factor  $(1 \pm \cos \theta_+)/2$ , which derives from the Berry phase structure of the graphene Hamiltonian. Furthermore, the nonlinear susceptibility Eq. (2) is not directly proportional to the imaginary part of the polarizability  $\Pi_i$  as in regular 2DEGs, because here the current  $\tilde{J}(\mathbf{k})$  is not directly proportional to the momentum  $\mathbf{k}$ . Equation (2) has the same formal structure as in the case of a regular 2DEG with Rashba or Dresselhaus spin-orbit coupling,<sup>13</sup> where  $\lambda = \pm 1$  describes the two spin-split bands. We consider the Coulomb drag between intrinsic graphene layers and extrinsic graphene layers separately.

*Drag in intrinsic graphene systems.* For the case where at least one of the graphene layers is undoped (i.e.,  $\mu = 0$ ), the drag conductivity is zero. This is not, as might be concluded at first sight, a trivial consequence of zero doping, as there is

a nonzero conductivity (the so-called ‘‘minimum conductivity’’) at zero doping in graphene. Hence a physical explanation and mathematical argument for why  $\sigma_D = 0$  is in order. When the Fermi level is at the Dirac point, the only process for electron-hole pair creation will be interband electron excitation from the valence band to the conduction band by which equal numbers of electrons and holes are created. In the mechanism of Coulomb drag, the applied electric field drives the electrons (or holes) in the active layer in the, say, positive (negative) direction; through Coulomb scattering, momentum is transferred to the passive layer, which drives the carriers (regardless of whether these are electrons or holes) in the same direction as the momentum transfer. In doped systems where there is only one type of carrier (either electrons or holes), this gives a finite drag current in the passive layer. In undoped systems where electron-hole symmetry exists, there are two cases for consideration. (i) If the active layer is undoped, equal numbers of electrons and holes in the active layer will be driven in the opposite direction by the applied electric field, and hence the net momentum transfer is thus zero. There will be no drag regardless of what the passive layer is. (ii) If the active layer is doped while the passive layer is undoped, equal numbers of electrons and holes in the passive layer will be driven in the same direction by the momentum transfer, therefore resulting in a vanishing drag current. These considerations lead us to expect that  $\Gamma(\mathbf{q}, \omega)$  vanishes for  $\mu = 0$ , which we prove as follows. We first make a change of the integration variable  $\mathbf{k}' = -\mathbf{k}$  in Eq. (2), and then apply time-reversal symmetry to the resulting expression. So far, this is general. Next we impose the symmetry requirements of the bands about  $\epsilon = 0$ ; i.e.,  $\epsilon_{k'\lambda} = -\epsilon_{k',-\lambda}$  and  $\tilde{J}_{\lambda\lambda}(\mathbf{k}') = -\tilde{J}_{-\lambda,-\lambda}(\mathbf{k}')$ , and then change the band labels as  $r' = -\lambda$ ,  $r = -\lambda'$  in the resulting expression. Finally, using the relation  $n_F(\epsilon_{k',-r}) = 1 - n_F(\epsilon_{k',r})$  (where  $n_F$  is the Fermi distribution function), valid for the undoped case  $\mu = 0$ , we arrive at  $\Gamma = -\Gamma$ , i.e.,  $\Gamma(\mathbf{q}, \omega) \equiv 0$ . This result holds true for any type of spectrum where the two bands have a mirror symmetry across  $\epsilon = 0$ , and any double-layer system with one or both of the layers having such a band symmetry with zero doping always results in an overall vanishing drag at all temperatures.

*Drag in extrinsic graphene systems.* The nonlinear susceptibility Eq. (2) for Fermi energy  $\epsilon_F > 0$  and  $T = 0$  is [in the following,  $x = q/k_F$  where  $k_F$  is the Fermi wave vector,  $y = \omega/\epsilon_F$ , and  $\tilde{\Gamma} = \Gamma / (2ek_F\tau/\pi)$ ]:  $\tilde{\Gamma}(x, y) = \tilde{\Gamma}_{\text{intra}}\theta(x-y) + \tilde{\Gamma}_{\text{inter}}\theta(y-x)$ , where  $\theta$  is the unit step function,  $\tilde{\Gamma}_{\text{intra}}$  is the intraband contribution given by the terms with  $\lambda = \lambda'$  in Eq. (2),

$$\tilde{\Gamma}_{\text{intra}}(x, y) = \frac{1}{4x} \sqrt{x^2 - y^2} \left\{ 2\sqrt{(y+x-2)(y-x-2)} - \sqrt{x^2 - y^2} \right. \\ \left. \times \left[ \tan^{-1} \left( \frac{\sqrt{(y+x-2)(y-x-2)}\sqrt{x^2 - y^2}}{x^2 - 2 - (y-2)y} \right) + \pi\theta[y(y-2) - x^2 + 2] \right] \right\} \theta(2-x-y) - \{y \rightarrow -y\}, \quad (3)$$

and  $\tilde{\Gamma}_{\text{inter}}$  is the interband contribution given by the terms with  $\lambda \neq \lambda'$  in Eq. (2),

$$\begin{aligned} \tilde{\Gamma}_{\text{inter}}(x,y) = & -\frac{1}{4x}\sqrt{y^2-x^2}\left\{2\sqrt{(x+y-2)(x-y+2)}+\sqrt{y^2-x^2}\right. \\ & \times \left[\tan^{-1}\left(\frac{\sqrt{(x+y-2)(x-y+2)}\sqrt{y^2-x^2}}{x^2-2-(y-2)y}\right)-\pi\theta[x^2-2-(y-2)y]\right]\left.\right\}\theta(x+y-2)\theta(x-y+2). \end{aligned} \quad (4)$$

For  $\varepsilon_F < 0$ ,  $\tilde{\Gamma} \rightarrow -\tilde{\Gamma}$  (with  $y = \omega/|\varepsilon_F|$ ), due to the symmetry of the conduction and valence bands about the Dirac point.<sup>14</sup>

The intraband contribution corresponds to electron-hole excitations in the vicinity of the Fermi level within the conduction band, which occur at  $\omega < vq$ ; whereas the interband contribution corresponds to electron-hole excitations from the valence band to the conduction band, which occur at  $\omega > vq$ . The drag resistivity  $\rho_D \approx -\sigma_D/(\sigma_{L1}\sigma_{L2})$  can be calculated using Eqs. (1), (3), and (4), and the expression for the graphene polarizability.<sup>4</sup> The longitudinal conductivities  $\sigma_L$  can be obtained from the impurity-dressed current  $\mathbf{J} = (\tau_{\text{tr}}/\tau)ev\hat{\sigma}$  using the Kubo formula, giving  $\sigma_L = e^2\nu D$ , where  $\nu = 2k_F/\pi v$  is the graphene density of states and  $D = v^2\tau_{\text{tr}}/2$  is the diffusion constant. There are two types of disorder in substrate-mounted graphene: charged impurities coming from the substrate, and neutral impurities intrinsic to the graphene layer itself. We emphasize that the presence of these different types of disorder in the graphene samples does not affect the expression of the drag resistivity as the transport time  $\tau_{\text{tr}}$  is explicitly canceled out between  $\sigma_D$  and  $\sigma_{L1}\sigma_{L2}$ . Therefore our calculation and conclusions apply equally to double-layer systems with substrate-mounted (where charged impurity scattering dominates) or suspended graphene samples (where there is only neutral impurity scattering).

It is instructive to obtain an analytical formula for the drag resistivity under certain approximations. To this end, we first define the dimensionless excitation energy  $u = y/x = \omega/vq$ . At low  $T$  and large  $d$ , the dominant contribution to the drag conductivity Eq. (1) comes from region with small  $q$  and  $\omega$ . Consequently  $\Gamma(\mathbf{q}, \omega)$  can be evaluated in the limits of long wavelength  $x \ll 1$  and low energy  $u \ll 1$ , allowing a closed-form expression for  $\Gamma(\mathbf{q}, \omega)$  to be extracted. The interband ( $\lambda \neq \lambda'$ ) contribution in Eq. (2) is in general smaller than the intraband ( $\lambda = \lambda'$ ) contribution by an order  $\mathcal{O}(x^2)$ , and vanishes in the limit  $u \ll 1$ . This is because, in the presence of a finite Fermi level, electrons take more energy to transition from the valence band to the conduction band (interband) than to transition within the conduction band (intraband), and with a small excitation energy the channel of interband transition becomes inaccessible. With the above assumptions, Eq. (2) can be evaluated yielding  $\tilde{\Gamma}(x, y = ux) = \tilde{\Gamma}_{\text{intra}} \approx -4ux$ .

In the expression of the drag conductivity Eq. (1), the dominant contribution of the integral comes from the region where  $qd \ll 1$ , and for large interlayer separation  $d$  satisfying  $d^{-1} \ll k_F, q_{\text{TF}}$ , the interlayer potential can be approximated as  $U_{12} \approx q/4\pi e^2 \sinh(qd)\Pi_1\Pi_2$ . Furthermore, the denominator  $\sinh^2(\omega/2k_B T)$  in Eq. (1) also restricts the upper limit of the  $\omega$  integral to a few  $\sim k_B T$ , therefore at low temperatures only small values of  $\omega$  contribute to Eq. (1). As a consequence,

the polarizability for doped graphene can be approximated by the static screening result  $\Pi(q, \omega) \approx \nu$ . Now, using  $\tilde{\Gamma} \approx -4ux$  for the nonlinear susceptibility, the drag resistivity is obtained as

$$\rho_D = -\frac{h}{e^2} \frac{\pi\zeta(3)}{32} \frac{(k_B T)^2}{\varepsilon_{F1}\varepsilon_{F2}} \frac{1}{(q_{\text{TF}1}d)(q_{\text{TF}2}d)} \frac{1}{(k_{F1}d)(k_{F2}d)}, \quad (5)$$

where  $q_{\text{TF}} = 4e^2k_F/v$  is the Thomas-Fermi wave number for extrinsic graphene.<sup>3</sup> The drag resistivity Eq. (5), valid for low temperatures  $T \ll T_F = \varepsilon_F/k_B$  and high density and/or large interlayer separation  $k_F d \gg 1$ , has exactly the same form as in the regular 2DEG drag, exhibiting the same dependences of temperature ( $\sim T^2$ ), interlayer separation ( $\sim 1/d^4$ ), and density ( $\sim (n_1 n_2)^{-3/2}$ ).

Figure 1 shows our numerical calculation and the analytical result, Eq. (5). It is evident that Eq. (5) becomes increasingly accurate as  $k_F d$  increases. The fact that the exact numerical results shown in Fig. 1 disagree more strongly with the analytic result for smaller values of  $k_F d$  is understandable, since Eq. (5) applies only in the  $k_F d \gg 1$  limit. This trend of an increasing quantitative failure of the asymptotic analytic drag formula for lower values of  $k_F d$  has also been noted in the literature<sup>15</sup> in the context of low-density hole drag in double-layer  $p$ -GaAs 2D systems. For small  $k_F d$ , backscattering effects in Coulomb drag, which are unimportant for  $k_F d \gg 1$ , become significant.

On the other hand, our numerical results also show that the temperature dependence of  $\rho_D$  remains very close to  $T^2$  within a wide range of temperatures for typical experimental values of  $d$  and  $n$  (e.g.,  $k_F d = 5$  with  $n = 5 \times 10^{11} \text{ cm}^{-2}$  and  $d \approx 400 \text{ \AA}$ ). The ratio of the Fermi temperature for graphene to that of a regular 2DEG with a parabolic spectrum (with

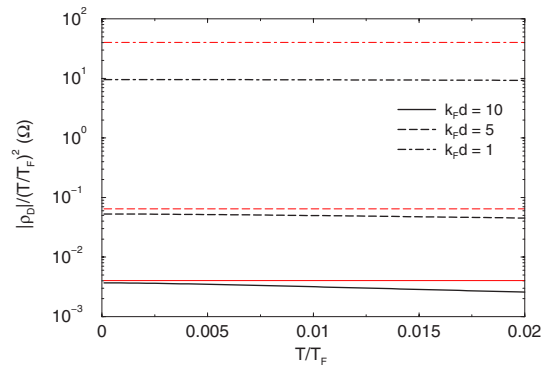


FIG. 1. (Color online)  $|\rho_D|/(T/T_F)^2$  as a function of  $T/T_F$  for Coulomb drag between two identical extrinsic graphene sheets, with values of  $k_F d = 10$  (solid lines), 5 (dashed lines), and 1 (dot-dashed lines). Numerical results are indicated with bold (black) lines and analytical results Eq. (5) with thin [grey (red)] lines.

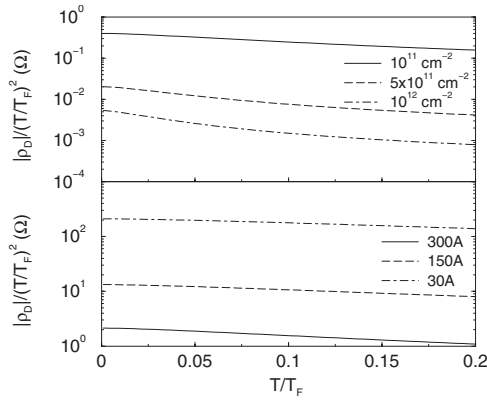


FIG. 2.  $|\rho_D|/(T/T_F)^2$  vs  $T/T_F$  for higher values of  $T$  up to  $0.2T_F$ . Upper panel: for fixed interlayer distance  $d=500$  Å and different values of density  $n=10^{11}$  cm $^{-2}$  (solid line),  $5 \times 10^{11}$  cm $^{-2}$  (dashed line),  $10^{12}$  cm $^{-2}$  (dot-dashed line), corresponding to  $T_F=431, 963, 1361$  K, respectively; lower panel: for fixed density  $n=10^{11}$  cm $^{-2}$  and different values of interlayer distance  $d=300$  Å (solid line),  $150$  Å (dashed line), and  $30$  Å (dot-dashed line).

effective mass  $m$ ) is  $mv/\hbar\sqrt{\pi n}$ . At a low density such as  $n=10^{11}$  cm $^{-2}$ ,  $T_F=430$  K for graphene is larger by an order of magnitude than  $T_F=42$  K for GaAs 2DEGs. Therefore the temperature dependence of  $\rho_D$  for graphene drag remains very close to  $T^2$  up to about several tens of kelvin since the low temperature regime  $T \ll T_F$  still remains valid, whereas for drag in GaAs 2DEG systems, departure from the  $T^2$  dependence of  $\rho_D$  typically occurs at  $T \lesssim 10$  K. The drag resistivity is calculated numerically for various values of  $d$  and  $n$  and higher values of temperature up to  $T=0.2T_F$  (Fig. 2);  $|\rho_D|$  is seen to grow slower than  $T^2$  as  $T$  increases. A similar dependence on  $T$  is also observed for drag in regular 2DEG double-layer systems before  $T$  reaches  $\approx 0.2T_F$ , beyond which  $|\rho_D|/T^2$  starts to increase due to plasmon enhancement to the drag resistivity.<sup>16</sup>

*Plasmon enhancement to extrinsic graphene drag.* In regular 2D double-layer systems, enhancement to the drag resistivity due to coupled plasmon modes comes into play with increasing temperature.<sup>16,17</sup> There exist two plasmon modes, the so-called optic and acoustic modes, for which the electrons on the two layers move collectively in phase and out of phase, respectively, with each other. The energy dispersion lines for these plasmon modes lie above the electron-hole excitation continuum (the region of  $\omega$ - $q$  space where the

imaginary part of the polarizability is nonzero) at  $T=0$ , and are not excited at low temperatures. They can be excited, however, at higher temperatures when the electron-hole excitation continuum occupies higher values of the excitation energy  $\omega$ , a consequence of the increasing gradient with increasing momentum  $k$  in the parabolic energy dispersion relation. Absorption or emission of a plasmon can occur when the electron-hole excitation continuum starts to overlap with the plasmon dispersion. On the other hand in graphene, since the gradient of the linear dispersion relation is constant, increasing temperature does not increase the range of the possible intraband excitation energies, the electron-hole excitation continuum being always bounded by  $\omega < vq$ . This means that the plasmon excitation energy will always be out of reach for the intraband excitation channel at all temperatures. However, the case is different with the interband excitation, for which the electron-hole excitation continuum overlaps plasmon dispersion already at  $T=0$  at about<sup>4</sup>  $\omega \gtrsim \epsilon_F$ . This means that plasmon-induced enhancement of the drag resistivity in graphene occurs solely in interband transitions, at a temperature  $T \gtrsim T_F$ ; whereas for regular 2D systems plasmon-induced enhancement occurs well before  $T$  reaches  $T_F$  (at about  $T \gtrsim 0.2$  to  $0.3T_F$ ). The coupled plasmon modes in graphene double-layer systems can therefore be probed experimentally with drag resistivity measurements at high enough temperatures or at low densities in clean samples.

*Conclusion.* We have theoretically studied Coulomb drag in graphene double layers. The drag resistivity is zero when at least one of the layers is intrinsic. For extrinsic graphene, the contribution to the drag due to interband electron-hole excitations is suppressed at low temperatures, and the Coulomb drag is due predominantly to the intraband contribution near the Fermi surface. For  $T \ll T_F$ , and  $k_F d \gg 1$ , the temperature, density, and distance dependence of  $\rho_D$  is the same as for parabolic-band 2DEGs. Plasmon-induced enhancement of the graphene drag resistivity does not occur at all for intraband excitations, in contrast to parabolic-band 2D double-layer systems, and it occurs in interband excitations only at temperatures  $k_B T \gtrsim \epsilon_F$ .

At this point, we note that it has recently come to our attention that an alternative description of Coulomb drag has appeared in the literature.<sup>18</sup>

*Acknowledgments.* We thank A. P. Jauho for useful comments on a draft of this paper. This work was supported by US-ONR.

<sup>1</sup>K. S. Novoselov *et al.*, Nature (London) **438**, 197 (2005); Y. Zhang *et al.*, *ibid.* **438**, 201 (2005).

<sup>2</sup>See, e.g., A. K. Geim and K. S. Novoselov, Nat. Mater. **6**, 183 (2007), and references therein.

<sup>3</sup>S. Das Sarma *et al.*, Phys. Rev. B **75**, 121406(R) (2007).

<sup>4</sup>E. H. Hwang and S. Das Sarma, Phys. Rev. B **75**, 205418 (2007).

<sup>5</sup>K. S. Novoselov *et al.*, Science **315**, 1379 (2007).

<sup>6</sup>S. V. Morozov *et al.*, Phys. Rev. Lett. **97**, 016801 (2006).

<sup>7</sup>T. J. Gramila *et al.*, Phys. Rev. Lett. **66**, 1216 (1991).

<sup>8</sup>U. Sivan *et al.*, Phys. Rev. Lett. **68**, 1196 (1992).

<sup>9</sup>H. Rubel *et al.*, Supercond. Sci. Technol. **10**, 1229 (1995).

<sup>10</sup>A.-P. Jauho and H. Smith, Phys. Rev. B **47**, 4420 (1993).

<sup>11</sup>A. Kamenev and Y. Oreg, Phys. Rev. B **52**, 7516 (1995).

<sup>12</sup>K. Flensberg *et al.*, Phys. Rev. B **52**, 14761 (1995).

<sup>13</sup>W.-K. Tse and S. Das Sarma, Phys. Rev. B **75**, 045333 (2007).

<sup>14</sup>A. Alkauskas *et al.*, Phys. Rev. B **66**, 201304 (2002).

<sup>15</sup>E. H. Hwang *et al.*, Phys. Rev. Lett. **90**, 086801 (2003).

<sup>16</sup>K. Flensberg and Ben Yu-Kuang Hu, Phys. Rev. Lett. **73**, 3572 (1994); Phys. Rev. B **52**, 14796 (1995).

<sup>17</sup>N. P. R. Hill *et al.*, Phys. Rev. Lett. **78**, 2204 (1997); H. Noh *et al.*, Phys. Rev. B **58**, 12621 (1998).

<sup>18</sup>B. N. Narozhny, arXiv:0704.2611v1 (unpublished).